

# Effect of Geometrical Parameters on Natural frequencies of FGM Cylindrical shell with Holes under Various Boundary Conditions

Mostafa Ghayour, Mohammad Sadegh Golabi

**Abstract**—In the recent years, functionally gradient materials (FGMs) have gained considerable attention in the high temperature environment applications. In this paper, free vibration of thin functionally graded cylindrical shell with hole composed of stainless steel and zirconia is studied. The mechanical properties vary smoothly and continuously from one surface to the other according to a volume fraction power-law distribution. The Influence of shell geometrical parameters, variations of volume fractions and boundary conditions on natural frequency is considered. The equations of motion are based on strains-displacement relations from Love's shell theory and Rayleigh method. The results have been obtained for natural frequencies of cylindrical shell with holes for different shape, number and location in this paper.

**Keywords**—functionally gradient material; Vibration; various boundary conditions; cylindrical shells;

## I. INTRODUCTION

THE functionally graded materials (FGMs) are microscopically inhomogeneous advanced composites with mechanical properties that vary continuously through a given dimension. In recent years, FGMs, especially metal-ceramic composites, have generated a great deal of interest in the aerospace community. This is due to their potential flexibility for use in the structural applications where extreme thermal, corrosion resistance and high-quality mechanical properties are required. In addition, FGMs have been widely used in various fields including electronics, chemistry, optics, biomedicine, etc. In regards to the material advances, because of the superior properties of advanced composite materials, such as specific strength and high specific stiffness, greater corrosion resistance, greater fatigue life due to material properties are graded in continuous direction. However, laminated composite structures exhibit serious risk of the delamination bonds at their interface of material layers when they are open to high-temperature environment. They are also easily affected by buckling, large amplitudes, and excessive stresses induced by thermal or combined thermo-mechanical loading. The design idea of FGMs was first introduced in 1984 by a group of Japanese materials scientists as a means of preparing thermal barrier materials [1]. FGMs are usually made by combining different materials using powder metallurgy methods [2]. Cylindrical shells also have vast range of applications in engineering and technology.

Ootao et al. have carried out studies on volume fraction optimization for minimizing thermal stresses in FGM hollow circular cylinder [3]. Kadoli et al. presented information for a better combination of metal and ceramic for FGM shell and also the magnitude of power-law index required for better thermal buckling characteristics [4]. Loy et al. investigated the free vibration of simply supported FGM cylindrical shells [5]. Pradhan et al. have studied vibration characteristics of a functionally graded cylindrical shell made up of stainless steel and zirconia for various boundary conditions. Effects of the boundary conditions and the volume fractions on the shell frequencies are analyzed [6]. Shah et al. have investigated vibration frequencies of cylindrical shells with the exponential volume fraction law [7]. Patel et al. analyzed free vibration of FGM elliptical cylindrical shells using Finite Element Method (FEM) based on higher-order Shear Deformation Theory (HSDT) [8]. Zhi-yuan and Hau-ning have studied the free vibration of FGM cylindrical shells with hole. Their analysis is based on Hamilton's principle [9]. Shahsiah and Eslami used Sanders nonlinear strain-displacement relation and first-order shell theory to derive the equilibrium and stability equations for a functionally graded cylindrical shell [10]. In this paper, the free vibration of a functionally graded cylindrical shell with hole is considered. Further, effect of the geometrical parameters, number of holes and the boundary conditions on the frequency characteristics of the FGM shells are studied. The analysis of the functionally graded cylindrical shell is carried out using Love's shell theory and solved by using Rayleigh method. The functionally gradient material considered is composed of stainless steel at the outer surface and zirconia at the inner surface.

## II. MATERIAL MODELS OF FUNCTIONALLY GRADED MATERIALS

The properties in a FGM shell change through the thickness, consequently. FGMs can potentially provide designers with tailored material response and exceptional performance in thermal environments and their material properties are temperature dependent. The material properties  $P_i$  can be expressed as a function of temperature [11]

$$P_i = P_0 (P_{-1} T^{-1} + 1 + P_1 T + P_2 T^2 + P_3 T^3) \quad (1)$$

Mostafa Ghayour is with Isfahan University of Technology, Iran (e-mail: sadegh\_golabi@yahoo.com)

Where  $P_0, P_{-1}, P_1, P_2$  and  $P_3$  are the coefficients of temperature  $T(Kelvin)$  and are unique to the constituent materials. The material properties  $P_{fgm}$  of FGMs are controlled by volume fractions  $V_f$  and individual material properties  $P_i$  of the constituent materials.

$$P_{fgm} = \sum_{i=1}^k P_i V_{fi} \quad (2)$$

Where

$$\sum_{i=1}^k V_{fi} = 1 \quad (3)$$

The volume fraction varies according to a simple power law function of the distance from middle surface of the cylindrical shell as follows,

$$V_{fi} = ((z + h/2)/h)^N \quad (4)$$

Where  $h$  is the cylinder wall thickness,  $N$  is the volume fraction index, and  $z$  is the coordinate in the radial direction ( $-h/2 \leq z \leq h/2$ ) with origin at the mid-surface, as shown in Fig.1

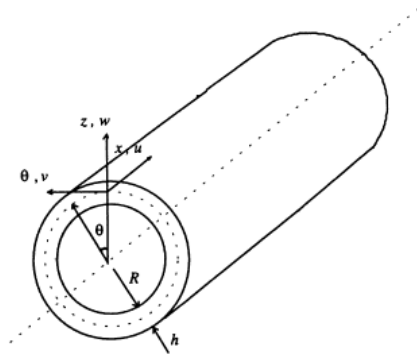


Fig. 1 Geometry of a cylindrical shell

For a functionally gradient material with two constituent materials, the Young's moduli ( $E_{fgm}$ ), Poisson's ratio ( $\nu_{fgm}$ ), and mass density ( $\rho_{fgm}$ ) for the materials M1 (Zirconia) and M2 (Stainless steel), respectively are expressed as

$$E_{fgm} = (E_2 - E_1) \cdot ((2z + h)/2h)^N + E_1 \quad (5)$$

$$\nu_{fgm} = (\nu_2 - \nu_1) \cdot ((2z + h)/2h)^N + \nu_1 \quad (6)$$

$$\rho_{fgm} = (\rho_2 - \rho_1) \cdot ((2z + h)/2h)^N + \rho_1 \quad (7)$$

The materials in outer  $z = h/2$  and inner  $z = -h/2$  surfaces of the cylindrical shell are stainless steel and zirconia, respectively. The material properties of FGM constituents, calculated at  $T = 300(K)$ , are listed in Table 1.

### III. STRAIN RELATIONS, FORCES AND MOMENTS RESULTANT

A cylindrical shell with radius  $R$ , length  $L$ , thickness  $h$  and square hole with dimensions  $d1, d2$  (Fig. 2) is considered for the present analysis. The deformations defined with reference to a coordinate system  $(x, \theta, z)$ .

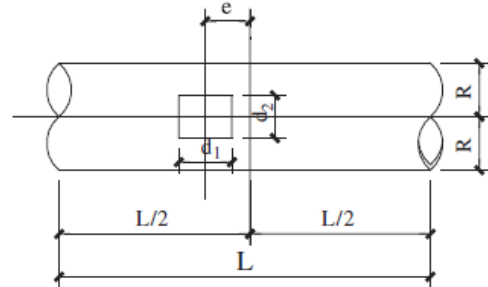


Fig. 2 Cylindrical shell with hole.

For a thin cylindrical shell, plane stress condition is assumed and the constitutive relation is given by

$$\{\sigma\} = [Q]\{e\} \quad (8)$$

Where  $\{\sigma\}$  and  $\{e\}$  represent stress and strain vectors and  $[Q]$  is the reduced stiffness matrix. The stress and strain vectors are defined as

$$\{\sigma\}^T = \{\sigma_x, \sigma_\theta, \sigma_{x\theta}\} \quad (9)$$

$$\{e\}^T = \{e_x, e_\theta, e_{x\theta}\} \quad (10)$$

Where  $\sigma_x$  and  $\sigma_\theta$  are the stresses in  $x$  and  $\theta$  directions, and  $\sigma_{x\theta}$  is the shear stress on the  $x\theta$  plane,  $e_x$  and  $e_\theta$  are the strains in the  $x$  and  $\theta$  directions, and  $e_{x\theta}$  is the shear strain on the  $x\theta$  plane. The reduced stiffness matrix is defined as

$$[Q] = \begin{bmatrix} Q_{11} & Q_{12} & 0 \\ Q_{12} & Q_{22} & 0 \\ 0 & 0 & Q_{66} \end{bmatrix} \quad (11)$$

For isotropic materials the reduced stiffness  $Q_{ij}$  are defined

$$Q_{11} = Q_{22} = \frac{E}{1-\nu^2}, \quad Q_{12} = \frac{\nu E}{1-\nu^2}, \quad Q_{66} = \frac{E}{2(1+\nu)} \quad (12)$$

TABLE I  
 MATERIAL PROPERTIES OF FGMS FROM REF. [12]

| Coefficient | Zirconia         |          |              | Stainless steel  |           |              |
|-------------|------------------|----------|--------------|------------------|-----------|--------------|
|             | $\rho(Kgm^{-3})$ | $\nu$    | $E(Nm^{-2})$ | $\rho(Kgm^{-3})$ | $\nu$     | $E(Nm^{-2})$ |
| P0          | 5700             | 0.2882   | 2.44E+11     | 8166             | 0.3262    | 2.01E+11     |
| P-1         | 0                | 0        | 0            | 0                | 0         | 0            |
| P1          | 0                | 1.13E-04 | -1.37E-03    | 0                | -2.00E-04 | 3.08E-04     |
| P2          | 0                | 0        | 1.21E-06     | 0                | 3.80E-07  | -6.53E-07    |
| P3          | 0                | 0        | -3.68E-10    | 0                | 0         | 0            |
| total       | 5700             | 0.298    | 1.68E+11     | 8166             | 0.3178    | 2.08E+11     |

From Love's shell theory [13], the components in the strain vector  $\{e\}$  are defined as

$$\begin{aligned} e_x &= e_1 - z\kappa_1 \\ e_\theta &= e_2 - z\kappa_2 \\ e_{x\theta} &= \gamma - 2z\tau \end{aligned} \quad (13)$$

Where  $e_1$ ,  $e_2$  and  $\gamma$  are the reference surface strains and  $\kappa_1$ ,  $\kappa_2$  and  $\tau$  are the surface curvatures. These surface strains and curvatures are taken from Love's shell theory

$$\{e_1, e_2, \gamma\} = \left\{ \frac{\partial u}{\partial x}, \frac{1}{R} \left( \frac{\partial v}{\partial \theta} + w \right), \frac{\partial v}{\partial x} + \frac{1}{R} \frac{\partial u}{\partial \theta} \right\} \quad (14)$$

$$\{\kappa_1, \kappa_2, \tau\} = \left\{ \frac{\partial^2 w}{\partial x^2}, \frac{1}{R^2} \left( \frac{\partial^2 w}{\partial \theta^2} - \frac{\partial v}{\partial \theta} \right), \frac{1}{R} \left( \frac{\partial^2 w}{\partial x \partial \theta} - \frac{\partial v}{\partial x} \right) \right\} \quad (15)$$

The forces and moments resultant expressed in terms of the stress components through the thickness

$$\{N_x, N_\theta, N_{x\theta}\} = \int_{-h/2}^{h/2} \{\sigma_x, \sigma_\theta, \sigma_{x\theta}\} dz \quad (16)$$

$$\{M_x, M_\theta, M_{x\theta}\} = \int_{-h/2}^{h/2} \{\sigma_x, \sigma_\theta, \sigma_{x\theta}\} z dz \quad (17)$$

Substituting Eqs. (8) and (13) into Eqs. (16) and (17) following constitutive equation is obtained

$$\{N\} = [S]\{\epsilon\} \quad (18)$$

Where  $\{N\}$ ,  $\{\epsilon\}$  and  $[S]$  are defined as

$$\{N\}^T = \{N_x, N_\theta, N_{x\theta}, M_x, M_\theta, M_{x\theta}\} \quad (19)$$

$$\{\epsilon\}^T = \{e_1, e_2, \gamma, \kappa_1, \kappa_2, 2\tau\} \quad (20)$$

$$[S] = \begin{bmatrix} A_{11} & A_{12} & 0 & B_{11} & B_{12} & 0 \\ A_{12} & A_{22} & 0 & B_{12} & B_{22} & 0 \\ 0 & 0 & A_{66} & 0 & 0 & B_{66} \\ B_{11} & B_{12} & 0 & D_{11} & D_{12} & 0 \\ B_{12} & B_{22} & 0 & 0 & D_{22} & 0 \\ 0 & 0 & B_{66} & 0 & 0 & D_{66} \end{bmatrix} \quad (21)$$

Where  $A_{ij}$ ,  $B_{ij}$  and  $D_{ij}$  are the extensional, coupling and bending stiffness, respectively, defined as

$$\{A_{ij}, B_{ij}, D_{ij}\} = \int_{-h/2}^{h/2} Q_{ij} \{1, z, z^2\} dz \quad (22)$$

#### IV. ENERGY RELATIONS

The Rayleigh approach is employed to obtain the equations of motion for a cylindrical shell. The Lagrangian energy functional  $\Pi$  for a shell is defined as the difference between the kinetic and strain energies and is given by

$$\Pi = T_{MAX} - U_{MAX} \quad (23)$$

Where  $T_{MAX}$  and  $U_{MAX}$  are the maximum kinetic and strain energies, respectively. The general expression for the kinetic energy of a circular cylindrical shell is given by

$$T = \frac{1}{2} \int_0^L \int_0^{2\pi} \rho_T \left[ \left( \frac{\partial u}{\partial t} \right)^2 + \left( \frac{\partial v}{\partial t} \right)^2 + \left( \frac{\partial w}{\partial t} \right)^2 \right] R d\theta dx \quad (24)$$

Where  $\rho_T$  is the mass density per unit length defined as

$$\rho_T = \int_{-h/2}^{h/2} \rho dz \quad (25)$$

The strain energy functional is given by

$$U = \frac{1}{2} \int_0^L \int_0^{2\pi} \{\epsilon\}^T [S] \{\epsilon\} R d\theta dx \quad (26)$$

#### V. SOLUTION PROCEDURE

Spatial displacement field for a freely vibrating cylindrical shell with different boundary conditions can be expressed as

$$u = A \frac{\partial \phi(x)}{\partial x} \cos(n\theta) \sin(\omega t) \quad (27)$$

$$v = B \phi(x) \sin(n\theta) \sin(\omega t) \quad (28)$$

$$w = C \phi(x) \cos(n\theta) \sin(\omega t) \quad (29)$$

Where A, B and C are constants denoting the amplitudes of the vibration in the axial u, circumferential v and radial w directions. n and  $\omega$  denote the number of circumferential waves in mode shape and angular frequency of vibration, respectively. Further, axial modal function  $\phi(x)$  is written as

$$\phi(x) = C_1 \sin\left(\frac{\eta x}{l}\right) + C_2 \cos\left(\frac{\eta x}{l}\right) + C_3 \sinh\left(\frac{\eta x}{l}\right) + C_4 \cosh\left(\frac{\eta x}{l}\right) \quad (30)$$

Where the values of numbers  $C_1$ ,  $C_2$ ,  $C_3$  and  $C_4$  are associated with the edge conditions described at the shell ends, and  $\eta$  is a real number corresponding to the eigenvalues of the beam function and is related with the axial wave number (m). Applying physical constraints on the axial displacements and their derivatives yields the following feasible boundary conditions specified at the ends,  $x = 0$  and  $x = L$ ,

$$\phi(x) = \frac{\partial \phi}{\partial x} = 0 \quad (\text{Clamped}) \quad (31)$$

$$\phi(x) = \frac{\partial^2 \phi}{\partial x^2} = 0 \quad (\text{Simply Supported}) \quad (32)$$

$$\frac{\partial^2 \phi}{\partial x^2} = \frac{\partial^3 \phi}{\partial x^3} = 0 \quad (\text{Free}) \quad (33)$$

To derive the frequency equation, the Lagrange function is minimized with respect to the amplitude coefficients A, B, and C. This leads to a set of three homogeneous simultaneous equations

$$\frac{\partial \Pi}{\partial A} = \frac{\partial \Pi}{\partial B} = \frac{\partial \Pi}{\partial C} = 0 \quad (34)$$

Performing the minimization as in Eq. (33) yields a set of equations that can be expressed as follows

$$\begin{bmatrix} C_{11} & C_{12} & C_{13} \\ C_{12} & C_{22} & C_{23} \\ C_{13} & C_{23} & C_{33} \end{bmatrix} \begin{bmatrix} A \\ B \\ C \end{bmatrix} = \begin{bmatrix} 0 \\ 0 \\ 0 \end{bmatrix} \quad (35)$$

The coefficients C11, C12 . . . C33 for a simply supported (SS-SS) boundary condition are listed in the Appendix. In order to solve its non-zero solution, the determinant of coefficient  $[C_{ij}]$  must be zero, the frequency equation can be obtained as

$$\alpha_0 \omega^6 + \alpha_1 \omega^4 + \alpha_2 \omega^2 + \alpha_3 = 0 \quad (36)$$

Where,  $\alpha_i$  (i = 0, 1, 2, 3) are constants and depend on material properties (E,  $\nu$ ,  $\rho$ ), geometrical parameters (R, L, h) and waves numbers (n, m). Eq. (36) is solved to yield three natural frequencies. The smallest of the three natural frequencies is interest to the present study.

#### VI. RESULTS AND DISCUSSIONS

Studies on vibration of FGM cylindrical shell with various boundary conditions are carried out. Natural Frequency for the FGM shell with and without hole for four boundary conditions is listed in Tables 2a and 2b.

TABLE II A.  
 VARIATION OF NATURAL FREQUENCIES (Hz) AGAINST CIRCUMFERENTIAL WAVE NUMBER FOR VARIOUS BOUNDARY CONDITIONS (m=1, h: R: L=1:20:60, N=1)

| n  | Boundary conditions |           |           |           |
|----|---------------------|-----------|-----------|-----------|
|    | S-S                 | C-C       | C-S       | C-F       |
| 1  | 16.171196           | 22.299541 | 19.464628 | 8.3449674 |
| 2  | 8.1702022           | 12.817861 | 10.569889 | 3.8507581 |
| 3  | 6.8004106           | 9.3559708 | 7.9774615 | 5.2233481 |
| 4  | 10.073866           | 10.981151 | 10.376087 | 9.3836409 |
| 5  | 15.509753           | 15.814426 | 15.524134 | 14.998232 |
| 6  | 22.374845           | 22.479015 | 22.294655 | 21.901716 |
| 7  | 30.535261           | 30.561846 | 30.417192 | 30.069811 |
| 8  | 39.962697           | 39.953862 | 39.826385 | 39.497387 |
| 9  | 50.649988           | 50.622511 | 50.503518 | 50.18302  |
| 10 | 62.595081           | 62.556587 | 62.442309 | 62.126216 |

TABLE II B.  
 VARIATION OF NATURAL FREQUENCIES (Hz) AGAINST CIRCUMFERENTIAL WAVE NUMBER OF FGM CYLINDRICAL SHELL WITH HOLE FOR VARIOUS BOUNDARY CONDITIONS (m=1, h: R: L=1:20:60, N=1)

| n  | Boundary conditions |           |           |           |
|----|---------------------|-----------|-----------|-----------|
|    | S-S                 | C-C       | C-S       | C-F       |
| 1  | 16.261357           | 22.302244 | 19.459267 | 8.3503894 |
| 2  | 8.2096594           | 12.818866 | 10.561945 | 3.8512663 |
| 3  | 6.8128365           | 9.3649302 | 7.9726433 | 5.222871  |
| 4  | 10.082657           | 10.982692 | 10.374538 | 9.3827253 |
| 5  | 15.519614           | 15.81508  | 15.523359 | 14.996968 |
| 6  | 22.385786           | 22.479455 | 22.293768 | 21.900155 |
| 7  | 30.546852           | 30.561834 | 30.416044 | 30.068017 |
| 8  | 39.974545           | 39.954881 | 39.825048 | 39.495442 |
| 9  | 50.661796           | 50.62248  | 50.502126 | 50.181013 |
| 10 | 62.606663           | 62.556622 | 62.440996 | 62.124233 |

In this paper studies are presented on the vibration of clamped-clamped (C-C) functionally graded (FG) cylindrical shells. In Fig. 3 illustrate fundamental frequency versus aperture ratio ( $\beta = d_2 / R$ ) of different FGM shells with middle square hole. It shows that the curve pattern is different for different shells. For slender shell (a), the shell with bigger hole has the less frequency; and the tubby shell (c) is reverse. For middle case (b), frequency is first reduced and increased then.

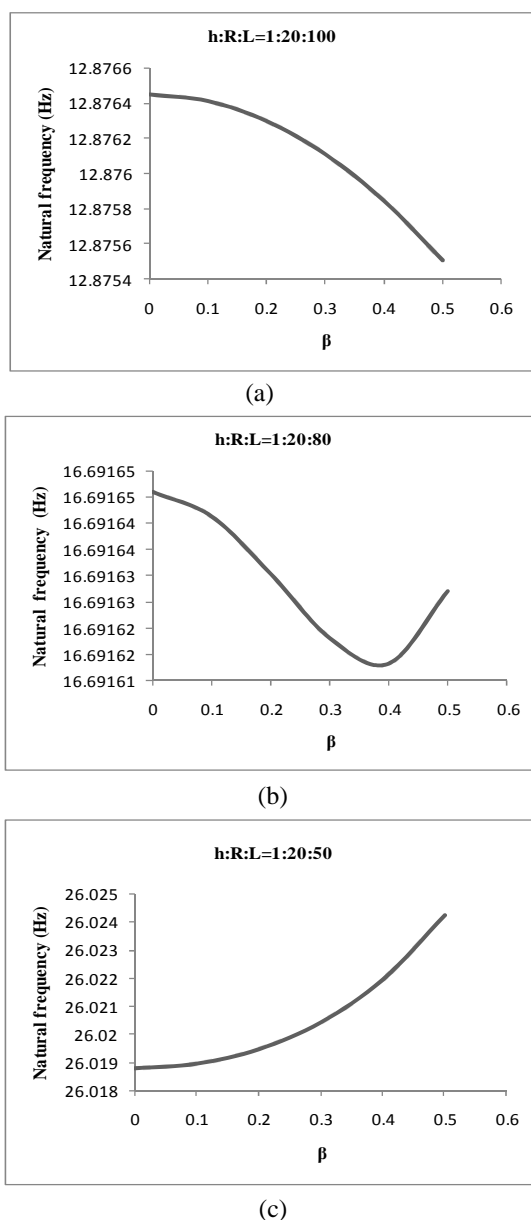


Fig. 3 Fundamental frequency versus aperture ratio. ( $m=1, N=1$ )

Fundamental frequency versus length–span ratio ( $\eta = R / L$ ) of FGM shells with middle square hole ( $h : R = 1 : 20, \beta = 0.4$ ) for different circumferential wave number ( $n$ ) is shown in Fig. 4. Table 3 gives the value of  $\omega$

and  $n$  of the lowest frequency (same  $\eta$ ). For the shorter shell (larger  $\eta$ ) and the same  $m$ ,  $\omega$  is not always increasing with  $n$ .

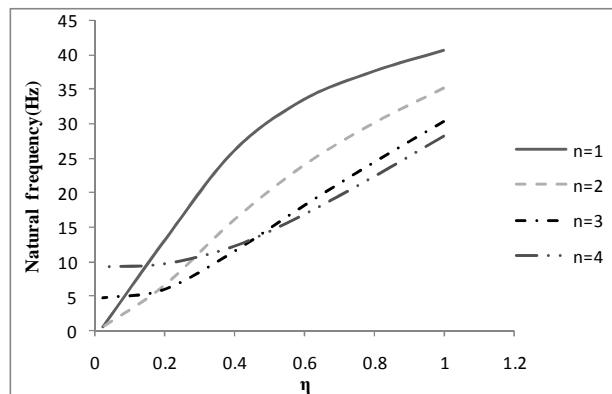


Fig. 4 Fundamental frequency versus length–span ratio

TABLE III  
 HIGH-FREQUENCY COEFFICIENT WITH RATIO OF LENGHT AND SPAN OF MIDDLE SQUARE HOLE

|                       |   | H        |          |          |          |          |
|-----------------------|---|----------|----------|----------|----------|----------|
| m                     | n | 0.025    | 0.1      | 0.2      | 0.4      | 0.6      |
| 1                     | 1 | 3.84E-01 | 4.822721 | 12.87550 | 26.02425 | 33.50546 |
|                       | 2 | 1.69E+00 | 2.523638 | 6.376213 | 15.90966 | 23.86286 |
|                       | 3 | 4.773937 | 4.905615 | 5.971117 | 11.48642 | 18.13591 |
|                       | 4 | 9.150680 | 9.215393 | 9.578131 | 12.12003 | 16.73229 |
| n of lowest frequency |   | n=1      | n=2      | n=3      | n=3      | n=4      |

In Fig. 5 is show fundamental frequency versus offsetting span ratio ( $\gamma = e / L$ ) of FGM shell with offset square hole. Frequency is first increased and reduced then.

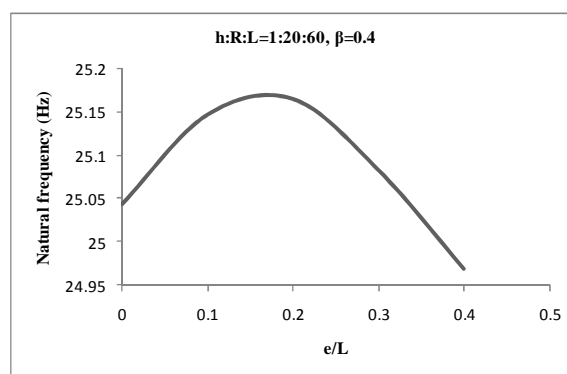


Fig. 5 Fundamental frequency versus offsetting span ratio of hole ( $m=1, N=1$ )

Fundamental frequency versus length–width ratio ( $\phi_p = d_2 / d_1$ ) of FGM shells with middle rectangular hole is shown in Fig. 6. Frequency is first reduced and increased then. In eneral when rectangular hole being groove in axial length frequency is reduced and when will be grooved in circumferential length frequency is increased.

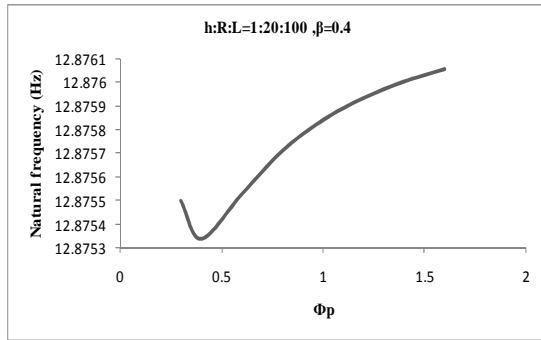


Fig. 6 Fundamental frequency versus length-width ratio of hole (m=1, N=1)

Fundamental frequency coefficient of FGM shell with multi-holes is shown in Fig. 7. When the holes distributed along circumferential or axial directions, the frequency is increasing with axial hole number. However, when hole number is even and holes distributed along circumferential, then fundamental frequency is smaller than odd number holes.

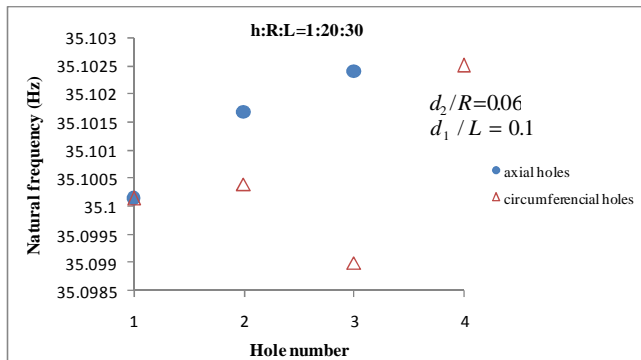


Fig. 7 Fundamental frequency coefficient of the shell with multi-holes (m=1, N=1)

## VII. CONCLUSIONS

In this study, the frequency analysis of thin functionally graded cylindrical shells with hole composed of stainless steel and zirconia has been presented. The equations of motion are based on Love's shell theory and solved by Rayleigh method. The maximum coupling stiffness occurs at N equals to 1 and the results are obtained for this power-law index. The influence of radius-span ratio, aperture ratio, offsetting, length-width ratio of hole and the numbers of holes on the natural frequency of functionally graded cylindrical shells is given by the numerical analyses. Results for the various boundary conditions are available (different boundary of  $\phi(x)$  in Eqs. (31) to (33)).

## APPENDIX

$$C_{11} = \frac{A_{11}m^2\pi^3R}{2L} + \frac{A_{66}\pi^2L}{2R} + \beta\omega^2$$

$$C_{12} = -\frac{mn\pi^2}{2} \left( A_{12} + A_{66} - \frac{B_{12}}{R} - \frac{B_{66}}{R} \right)$$

$$C_{13} = \frac{m\pi^2}{2} \left( -A_{12} + \frac{B_{11}n^2}{R} + \frac{2B_{66}n^2}{R} + \frac{B_{11}m^2\pi^2R}{L^2} \right)$$

$$C_{22} = \frac{m^2\pi^3}{2} \left( \frac{A_{66}R}{2} - B_{66} + \frac{D_{66}}{R} \right) + \frac{n^2L\pi}{R} \left( \frac{A_{22}}{2} - \frac{B_{22}}{R} + \frac{D_{22}}{2R^2} \right) + \beta\omega^2$$

$$C_{23} = \frac{m^2n\pi^3}{L} \left( -\frac{B_{12}}{2} - B_{66} + 2\frac{D_{66}}{R} \right) + \frac{n\pi L}{2R} \left( A_{22} - \frac{B_{22}}{R} \right) + \frac{n^3\pi L}{2R^3} \left( -B_{22} + \frac{D_{22}}{R} \right)$$

$$C_{33} = \frac{m^2n^2\pi^3}{LR} (D_{12} + 2D_{66}) + \frac{n^2\pi L}{R^2} \left( -B_{22} + \frac{D_{22}n^2}{2R} \right) + \frac{m^2\pi^3}{L} \left( -B_{12} + \frac{D_{11}m^2\pi^2R}{2L^2} \right) + \frac{A_{22}\pi L}{2R} + \beta\omega^2$$

Where

$$\beta = \frac{\pi\rho RL}{2}$$

## REFERENCES

- [1] Koizumi M., Functionally graded materials the concept of FGM. Ceramic Transactions, Vol (34), 1993;pp 3-10
- [2] Anon, FGM components: PM meets the challenge. Metal Powder Report, Vol 51, 1996; pp 28-32..
- [3] Ootao Y., Tanigawa Y., Nakamura T., Optimization of material composition of FGM hollow circular cylinder under thermal loading: a neural network approach, Composites Part B 30 (1999) 415-422.
- [4] Kadoli R., Ganesan N., Buckling and free vibration analysis of functionally graded cylindrical shells subjected to a temperature specified boundary condition, Journal of Sound and Vibration 289 (2006) 450-480.
- [5] Loy C.T., Lam K.Y., Reddy J.N., Vibration of functionally graded cylindrical shells, International Journal of Mechanical Sciences 41 (1999) 309-324
- [6] Prandhan S.C., Loy C.T., Lam K.Y., Reddy J.N., Vibration characteristics of FGM cylindrical shells under various boundary condition, Applied Acoustics 61 (2000) 111-129
- [7] Shah A.G., Mohmood T., Naeem M.N., Vibrations of FGM thin cylindrical shells with exponential volume fraction law, Applied Mathematics and Mechanics, 30(5), (2009), 607-615
- [8] Patel B.P., Gupta S.S., Moknath M.S., Free vibration analysis of FGM elliptical cylindrical shells, Composite Structure, 69, (2005), 259-270
- [9] Zhi-yuan C., Hua-ning W., Free vibration of FGM cylindrical shells with holes under various boundary conditions, Journal of Sound and Vibration 306 (2007) 227-237
- [10] Shahsiah R., Eslami M.R., Thermal buckling of functionally graded cylindrical shell, Journal of Thermal Stresses 26 (2003) 277-294.
- [11] Touloukian YS. Thermo physical properties of high temperature solid materials. New York: Macmillan, 1967.
- [12] Love AEH. A treatise on the mathematical theory of elasticity. 4th Ed. Cambridge: Cambridge University Press, 1952.
- [13] Roa S.S., Vibration of continuous systems, John Wiley & Sons, Inc., Hoboken, New Jersey, 2007, 540-605